

Robust Design of Kretschmann Plasmonic PCW-based Integrated Biosensor Circuit

Kalaivani A. Tarumaraja¹, P. Suthitha Menon^{1*}, Burhanuddin Yeop Majlis¹ and Prakash R. Apte²

¹*Institute of Microengineering and Nanoelectronics (IMEN), Universiti Kebangsaan Malaysia (UKM), 43600 UKM Bangi, Malaysia.*

²*Indian Institute of Technology at Bombay, Powai, Mumbai, India.*

Received 2 September 2018, Revised 12 October 2018, Accepted 12 November 2018

ABSTRACT

This paper presents the design optimization of an Integrated Biosensor Circuit (IBC) which utilizes graphene-based plasmonic Photonic Crystal Waveguide (PCW). The effects of 5 input signals, 4 control factors and 1 noise factor were investigated using Taguchi's dynamic L_9 orthogonal array where the input signals are linearly related to the output response. The focus is to find the best combination of the parameters to achieve the best linearity insensitive to noise and obtain a robust design of the IBC. The input signals are based on the Refractive Index (RI) of glucose concentration in urine which ranges from 1.335 to 1.341. The control factors of the IBC are the PCW length (μm) – Factor A, the waveguide Bragg grating (WBG) length (μm) – Factor B, the modulator P length (μm) – Factor C, and the modulator Q length (μm)-Factor D, whereas the noise factor is the delta temperature of modulator Q where each factor was evaluated at 3 level values. Taguchi's Higher-the-Better signal-to-noise (S/N) ratio was used to maximize the Free Spectral Range (FSR) of the IBC's reflection output power which will directly increase the IBC's biosensing sensitivity. The dominant control factors were identified as the PCW length (43% factor effect) and the WBG₂ length (22% factor effect). Upon dynamic Taguchi optimization, the FSR of the IBC improved by 0.62 dB for S/N ratio for linearity, the best control factors is A1B1C1D2, and the IBC's sensitivity improved to 8.86 μm /RIU for detection of glucose concentration in urine.

Keywords: Integrated Biosensor Circuit (IBC), Dynamic Taguchi Method (DTM), Signal-To-Noise Ratio (S/N), Photonic Crystal Waveguide (PCW), Surface Plasmon Resonance (SPR).

1. INTRODUCTION

Current advanced technology in the medical field provides a greater understanding of biomolecular interaction via increment of detection accuracy and precision measurement. For example, optical biosensors with Kretschmann-based Surface Plasmon Resonance (SPR) technique is able to detect lower concentrations fg/ml [1-5] of biomolecules based on the change in mass, Refractive Index (RI) or charge [6-12]. Besides that, Photonic Crystal Waveguide (PCW)-based biosensors are capable of detecting varieties of biotargets with high selectivity and efficiency with emerging technologies including flexible and smart nanomaterials such as Carbon Nanotubes (CNT), and graphene [13-19]. Generally, optical transduction in photonic biosensors is empowered by the sensitivity of an optical surface mode to change the RI. Current research is actively pursuing Integrated Biosensor Circuits (IBC) with the ability to combine optical light sources and detection devices completely on an operational silicon-based Lab-on-

* Corresponding Author: susi@ukm.edu.my

Chip (LOC) device with label-free detection for rapid Point-of-Care (POC) analysis [6, 20, 21]. This integration can be divided into two types; monolithic or hybrid where monolithic integration requires the whole system to be integrated on one chip whereas hybrid integration requires functionality to be carried out in more than one component that is finally combined on a single chip [22,23]. Integration can exploit a strong-density array of the photonic biosensor and IBCs can be built to control the penetration depth of the optical mode [6].

Normally, the design and improvement of a device rely heavily on experimental approaches. But, faulty apparatus or operational errors, is essentially unavoidable. Therefore, dissimilarity happens between the specifications of design and the outcome of experiments. The techniques of computer-aided design such as Lumerical's Finite Difference Time Domain (FDTD) and Interconnect contribute powerful tools of simulation for the challenge of designing complex optical structures prior to actual experimental work [9,10,24-28]. By implementing this technique, they facilitate coupled-field finite element which can provide analysis and efficient results of the prototype [29-30].

Taguchi method allows selected design parameters to be evaluated and ensures that a robust design of the simulation results and prototype is obtained. The dynamic characteristic such as noise or input signals can influence the accuracy of the measured signal [31-34]. In this paper, the optimal robust design was obtained based on the signal-to-noise ratio (linearity) of the Free Spectral Range (FSR) of the output reflection power signals from a plasmonic PCW IBC using Dynamic Taguchi Method.

2. MATERIALS AND METHODS

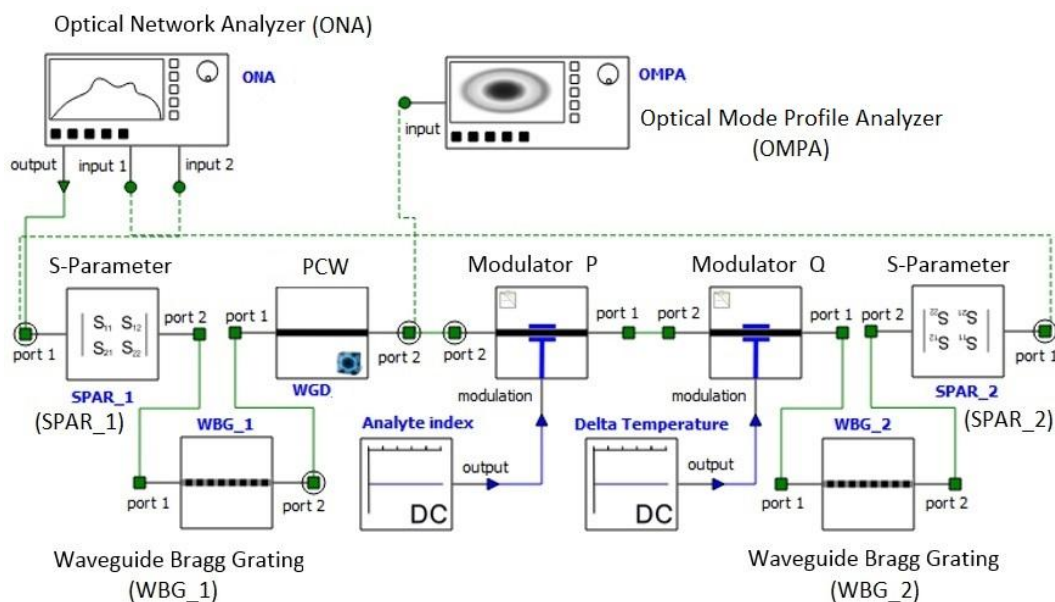


Figure 1. IBC design on INTERCONNECT.

a) IBC Simulation Design

The IBC was previously designed using Interconnect solver from Lumerical [35-37]. In this work, waveguide Bragg gratings were added as optical filters to the IBC in order to obtain better measurable results. The FSR of the optical reflection output signals were measured to correlate with the level of glucose concentration in urea. The IBC is shown in Figure 1. This IBC is

designed with a PCW which incorporates alternating multilayer metal oxide of Al_2O_3 with 250nm thickness, a non-metal oxide of SiO_2 with 300nm thickness, single layer graphene with one atom thickness, and Polymethyl-methacrylate (PMMA) of 100nm thickness [37]. The IBC also consist of waveguide Bragg gratings WBG_1 and WBG_2, electro-optic modulator P, electro-optic modulator Q, optical S-parameters SPAR_1 and SPAR_2, Optical Network Analyzer (ONA), and Optical Mode Profile Analyzer (OPMA). The main input power signal propagates from ONA with a frequency of 374.741GHz which was set based on the PCW wavelength. The output signal from SPAR_1 is connected to WBG_1 which acts as an optical filter to reduce noise and the output from WBG_1 is subsequently connected to PCW which acts as the biosensor. The PCW is connected to electro-optic modulators P and Q for signal modulation purposes. The electro-optic modulator P is connected to an optical phase shifter which adds a small shift in the effective index that depends on the RI of glucose concentration in urine which varies from 1.335 to 1.341. The second electro-optic modulator Q is connected to a second phase shifter element which represents the phase shift due to temperature changes. The default temperature is set at 300K. The output signal from electro-optic modulator Q will go through WBG_2 for signal filtration after the optical signal is modulated and propagates to SPAR_2. An output signal from SPAR_2 is connected to the ONA via input 1. The OMPA is connected to the PCW to view the TE optical mode in two dimensions. Figure 2 shows the reflection output power in TE mode of various RI with reference to the amount of glucose concentration in the urine sample for the PCW-based IBC. The FSR is measured from one peak to another of a particular sinusoidal wave corresponding to a particular RI as shown in Figure 2.

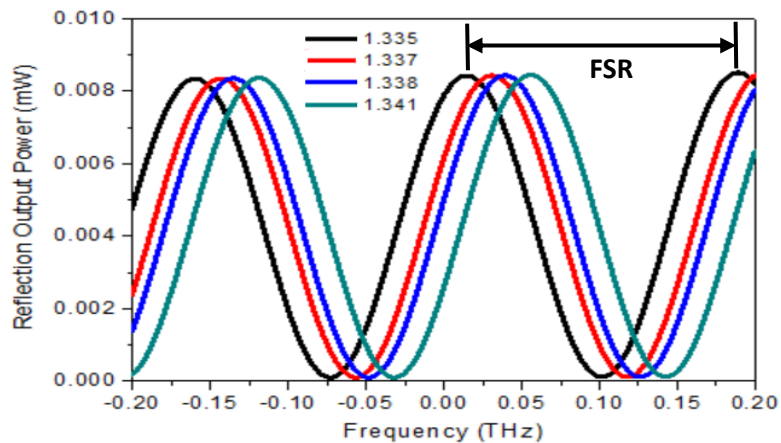


Figure 2. Reflection output power (mW) and FSR of the IBC [34].

b) Design of Experiment for Optimization of IBC via Dynamic Taguchi Method

The Dynamic Taguchi method is a form of fractional factorial design using orthogonal arrays. It is a fixed array based on the degrees of freedom approach. The dynamic Taguchi L_9 orthogonal array method requires four process parameters and one noise factor to complete the design of orthogonal array. It can be classified as a dynamic problem according to the nature of the quality characteristic and the signal factor as well as their relationship [38-40]. Figure 3 shows the dynamic measurement based on Taguchi method by a simplified presentation via a P-diagram [31].

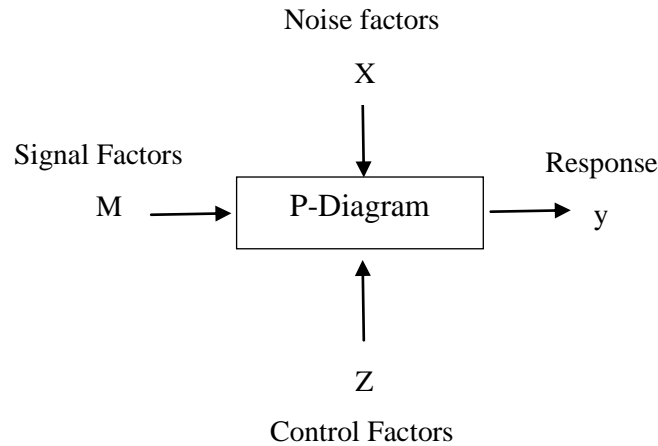


Figure 3. P-Diagram of Taguchi's dynamic analysis.

The dynamic Taguchi method S/N ratio in this work is “Higher-the-Better” or also known as “Larger-the-Better” for the output of the IBC is the FSR. The S/N ratios are calculated using Equation (3), where n is an observation number and Y is the observed data. The scale of S/N ratio is expressed using decibel (dB). Taguchi Method is capable of defining which process parameters are significant through the Analysis of Variance (ANOVA). The prediction of process parameters based on the optimal combination can be determined by the S/N ratio and ANOVA analyses as well as confirmation experiments. In considering a dynamic relationship, the output can be adjusted by changing the input signal factor expressed in a simple linear relationship equation which is between the response, Y , the signal factor, M , and the error, ε as in Equation (1) i.e. where the control factor is $i=1,2, I$, the signal factor is $j=1, 2, J$, and the noise factor is $k=1,2, r_o$ where y_{ijk} is the quality characteristic for M_j and noise condition. In order to find the correct adjustment for a given control setting, first, the slope of the best linear relationship between y_{ijk} and M_j must be estimated. The Least Squares Method (LSM) refers to the slope, β . The LSM minimizes the sum of the squares of the data and is expressed in Equation (2). The j th characteristic result of the experiment/simulation is y_{ijk} , the j th level input signal is M_j , the outer orthogonal array of experimental trial number is r_o , and the input signal of the level setting is j [31,38,41-43].

$$Y_{ijk} = \beta_i M_j + \varepsilon_{ijk} \quad (1)$$

$$\beta = [(\sum_{j=1}^J \sum_{k=1}^{r_o} y_{ijk} M_j) / r_o \sum_{j=1}^J M_j^2] \quad (2)$$

$$\frac{S}{N} = -10 \log \left(\frac{1}{n} \sum_{i=1}^n \frac{1}{Y_i^2} \right) \quad (3)$$

Many parameters can influence the quality characteristic of the product design. The dynamic L₉ Taguchi method implemented in this work has five (5) level of signal factors (M) for RI of glucose concentration levels in a sample of urine and one noise factor (X) which is the delta temperature connected to Modulator Q. The noise factor causes the response (y) which is the IBC's FSR to deviate from the target specified by the signal factor (M) and lead to quality loss.

The four (4) control factors (Z) varied at three levels are the PCW length, WBG_2 length, modulator P length, and modulator Q length. Control factors affect manufacturing cost as well as tolerance factors. The response Y is the FSR of the IBC reflection output wave corresponding to a particular RI. A larger FSR will give a better biosensor sensitivity to the IBC. The noise factors are included in order to get a more accurate design and to make the process parameters insensitive to noise. A total of 135 simulation experiments were run such that all factor

combinations are explored as required by the L_9 dynamic Taguchi method. All the values of the control factors, signal factors, noise factors and L_9 orthogonal array are shown in Table 1, Table 2 and Table 3. These values were selected with reference from previous works [44-47]. With reference to Figure 3, the RI refers to the signal factors, M as shown in Table 2, whereas the control factors, Z are shown in Table 1. For every RI value, the simulation is executed based on the orthogonal array in Table 3 for different control factor levels.

Table 1 Control factors (Z) for the dynamic Taguchi L_9 optimization

No.	Control Factors (Z)	Level 1		Level 2		Level 3	
1	PCW length (μm)	A1	300	A2	400	A3	500
2	WBG_2 length (μm)	B1	200	B2	300	B3	400
3	Modulator P length (μm)	C1	250	C2	350	C3	450
4	Modulator Q length (μm)	D1	100	D2	150	D3	200

Table 2 Signal factors based on RI of glucose concentration in urine and noise factor of delta temperature of modulator Q

Signal Factors (M)					Noise Factor (X), Delta Temperature (K)		
Refractive Index (RI)					Level 1	Level 2	Level 3
1.335	1.336	1.337	1.338	1.341	0	0.5	1.0

Table 3 L_9 dynamic Taguchi orthogonal array

Control Factors Assigned to columns				
Exp. No.	PCW Length (μm)	WBG_2 Length (μm)	Modulator P length (μm)	Modulator Q length (μm)
1	A1	B1	C1	D1
2	A1	B2	C2	D2
3	A1	B3	C3	D3
4	A2	B1	C2	D3
5	A2	B2	C3	D1
6	A2	B3	C1	D2
7	A3	B1	C3	D2
8	A3	B2	C1	D3
9	A3	B3	C2	D1

3. RESULTS AND DISCUSSION

The five (5) RI signals were simulated for each control factor combination for every noise factor level and the FSR response measurement was obtained from the reflection output power signal. By applying the given formula from Equation (1) - Equation (3), the S/N ratio for each FSR of the IBC was calculated and tabulated in Table 4.

Table 4 Main effects of linearity

Column No.		Main Effects (Linearity)											
		1			2			3			4		
Control factors		Wave Length (um)			Bragg Grating Length (um)			P Modulator_1 (um)			Q Modulator_2 (um)		
Exp. No	S/N Ratio	A1	A2	A3	B1	B2	B3	C1	C2	C3	D1	D2	D3
1	82.75	82.7			82.7			82.7			82.7		
		5			5			5			5		
2	82.31	82.3				82.3			82.3			82.3	
		1				1			1			1	
3	72.84	72.8					72.8			72.8			72.8
		4					4			4			4
4	75.28		75.2		75.2				75.2				75.2
			8		8				8				8
5	73.22		73.2			73.2				73.2	73.2		
			2			2				2	2		
6	72.65		72.6				72.6	72.6					72.6
			5				5	5					5
7	72.43			72.4	72.4					72.4		72.4	
				3	3					3		3	
8	71.08			71.0		71.0		71.0					71.0
				8		8		8					8
9	64.87			64.8			64.8		64.8		64.8		
				7			7		7		7		
Sum	667.4	237.	221.	208.	230.	227.	210.	226.	222.	218.	220.	227.	219.
	4	9	2	4	0	1	4	0	9	5	4	8	2
Factor Effects		79.3	73.7	69.4	76.6	75.6	70.1	75.3	74.3	72.8	73.4	75.9	73.0
		0	2	6	8	8	2	5	0	3	7	4	7

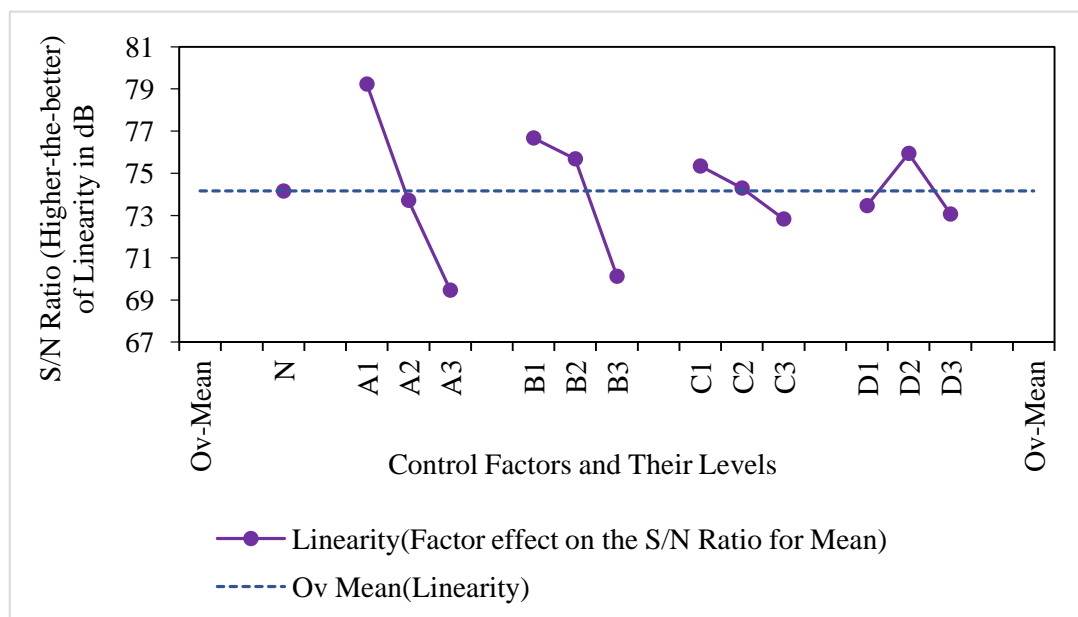


Figure 4. S/N ratio of Linearity in dB.

When the S/N ratio value is higher, the IBC has better performance characteristics. The highest S/N ratio for linearity (higher-the-better) is 82.75dB whereas the lowest value is 64.87dB, the overall mean is 74.16dB and the total sum of S/N ratio is 667.44dB. The effects of the main factor for each level in linearity of S/N ratio is shown in Figure 4. The dashed horizontal line in the chart represents the value of the overall mean of the S/N ratio for linearity.

Table 5 ANOVA of S/N ratio for linearity (Higher-the-better)

Factor	Control Factor	Degree of Freedom (DOF)	Sum of Square (SS)	Mean Square (Variance)	Factor Effect (%)	Factor Effect on Mean (%)
A	PCW Length	2	146	73	43	59.72
B	WBG_2 Length	2	75	37	22	30.56
C	Modulator P Length	2	10	5	3	4.17
D	Modulator Q Length	2	15	7	4	5.55

The results of ANOVA for the IBC are presented in Table 5. The results show that there are only 2 dominant factors for S/N linearity (Higher-the-better); PCW length (Factor A) with 43% effect followed by the waveguide Bragg grating 2 (WBG_2) length, and factor B with 22% effect on the FSR measurement. However, no adjustment factor can be identified as the S/N linearity for Factor C and D because the ANOVA for both factors is low; below 6%.

The final full recommendation for an optimized IBC is the control factors with level values of A1, B1, C1, and D2 as highlighted in Figure 4 and Table 6. These final parameters were then simulated with signal and noise factors in order to obtain the optimal results as stated in Table 6.

Table 6 Best predicted setting for IBC using dynamic L9 Taguchi method

Factor	Control Factors	Unit	Level	Best Value
A	PCW Length	μm	1	300
B	WBG_2 Length	μm	1	200
C	Modulator P Length	μm	1	250
D	Modulator Q Length	μm	2	150

Table 7 The comparison of the S/N ratio between the original design and Taguchi-optimized design

Quality Characteristics	Original design	Taguchi optimised design	Improvement
Linearity (dB)	76.2	76.82	0.62

The control factor level settings for the original design was A1, B1, C1, and D1 in comparison with the robust IBC design with control factor levels of A1, B1, C1, and D2. Table 7 shows improvement between the predicted and verified the outcome of S/N ratio for the original design versus the robust design of the IBC. The outcome proved that the S/N ratio and sensitivity of the IBC increased based on the Taguchi dynamic characteristic design process. Hence, the biosensor can detect smaller changes of RI within the FSR of the signal without a loss of precision. Figure 5 shows the result of the improvement between the original and robust design graphically. The percentage of improvement in FSR is about 14.5% for RI of 1.335. Apart from the improvement of FSR, this research also able to determine the dominant factors and best control factor combination that affect the IBC design. Improvement of the design factors and values to obtain a significant improvement will be continued in future work.

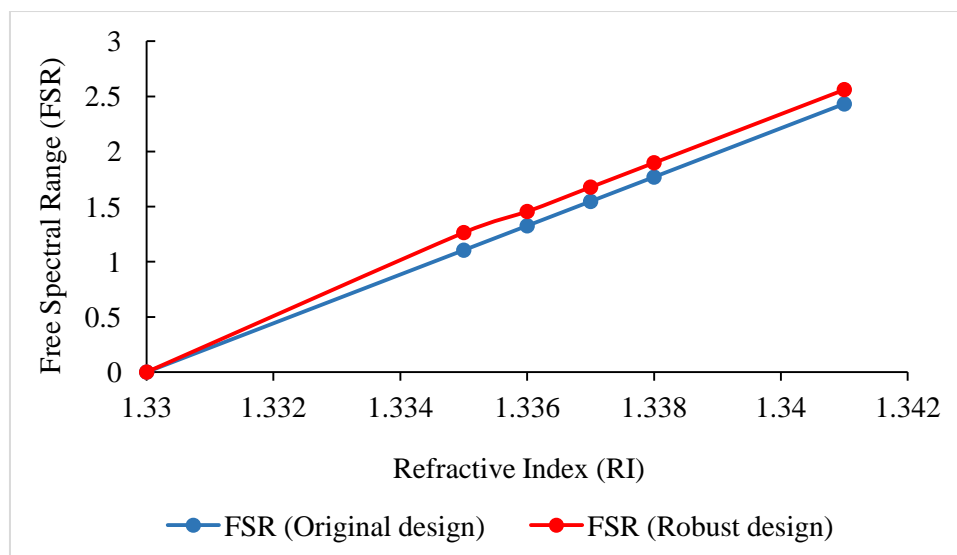


Figure 5. Comparison of original and robust design for IBC S/N ratio linearity analysis.

Meanwhile, the sensitivity of the original IBC design was $8.83\mu\text{m}/\text{RIU}$ and the Taguchi-optimized IBC design was $8.86\mu\text{m}/\text{RIU}$; higher than the sensitivity of $638\text{nm}/\text{RIU}$ reported previously [14]. Once the optimization approach was conducted, the value of the S/N ratio (higher-the-better) of FSR for the developed IBC showed that S/N ratio is within the predicted range of $79.00 - 83.20\text{dB}$. This indicates that the dynamic Taguchi Method can predict the best control factor combination in finding the robust design of the IBC with an appropriate FSR. The simulation shows that change in the length of PCW and waveguide Bragg grating directly affects the IBC's FSR of the reflection output power.

4. CONCLUSION

In conclusion, dynamic L_9 Taguchi method is a reliable method in achieving the optimum solution of robust design by identifying the main effects of control factors in a Kretschmann Plasmonic PCW-based IBC with the presence of signal and noise factors. The FSR of the reflection output power of the IBC was optimized using the S/N ratio of "higher-the-better". Upon optimization, a higher sensitivity value of $8.86\mu\text{m}/\text{RIU}$ was achieved for the detection of glucose concentration in urine. The main factors identified are PCW length and the waveguide Bragg grating length. The results indicate that the adopted methodology able to increase the sensitivity of the device while increasing the S/N ratio linearity.

ACKNOWLEDGEMENT

IMEN, UKM and the Ministry of Science, Technology and Innovation (MOSTI) are acknowledged for supporting this research with the National Impact Grant DIP-2016-022, Research University Grant GUP-2016-062 and MyBrain support.

REFERENCES

- [1] B. McDonnell, S. Hearty, P. Leonard & R. O'Kennedy, *Clinical Biochemistry* **42** (2009) 549-561.
- [2] R. Sharma, S. E. Deacon, D. Nowak, S. E. George, M. P. Szymonik, A. A. S. Tang, D. C. Tomlinson, A. G. Davies, M. J. McPherson & C. Walti, *Biosensors and Bioelectronics* **80** (2016) 607-613.
- [3] M. Durga Prakash, S. Vanjari, C. Sharma & S. Singh, *Sensors* **16** (2016) 1354.
- [4] J. Yuan, R. Oliver, M. Aguilar & Y. Wu, *Analytical Chemistry* **80** (2008) 8329-8333.
- [5] D. Maraldo, K. Rijal, G. Campbell & R. Mutharasan, *Analytical Chemistry* **79** (2007) 2762-2770.
- [6] J. Juan-Colás, S. Johnson & T. Krauss, *Sensors* **17** (2017) 2047.
- [7] F. A. Said, P. S. Menon, M. N. Nawi, A. R. Md Zain, A. Jalar & B.Y. Majlis, *Proc. IEEE International Conference on Semiconductor Electronics (ICSE)*, (2016) 264-267.
- [8] F. A. Said, P. S. Menon, V. Rajendran, S. Shaari & B. Y. Majlis, *IET Nanobiotechnology* **11** (2017) 981-986.
- [9] N. A. Jamil, P. S. Menon, F. A. Said, K. A. Tarumaraja, S. M. Gan & B. Y. Majlis, *Proc. IEEE Regional Symposium on Micro and Nanoelectronics (RSM)*, (2017) 112-115.
- [10] N. A. Jamil, P. S. Menon, S. M. Gan, S. Shaari & B. Y. Majlis, *IEEE Region 10 Conference TENCN*, (2017) 1973-1977
- [11] N. A. Jamil, P. S. Menon, S. M. Gan & B.Y. Majlis, *Sains Malaysiana* **47** (2018) 1033-1038
- [12] Fan, V. L. Siu & Y. Yusof, *Int. J. Nanoelectronics and Materials* **8** (2015) 55-50
- [13] H. Inan, M. Poyraz, F. Inci, M. A. Lifson, M. Baday, B. T. Cunningham & U. Demirci, *Chemical Society Reviews* **46** (2017) 366-388.
- [14] P. Russell. *Science* **299** (2003) 358-362.
- [15] H. Inan, M. Poyraz, F. Inci, M. Lifson, M. Baday, B. Cunningham & U. Demirci, *Chemical Society Reviews* **46** (2017) 366-388.
- [16] P. Sharma & P. Sharan, *IEEE Sensors Journal* **15** (2015) 1035-1042.
- [17] S. Robinson & N. Dhanalaksmi, *Photonic Sensors* **7** (2017) 11-19.
- [18] M. A. Shazni, M. W. Lee & H. W. Lee. *Sains Malaysiana* **46** (2017) 1155-1161.
- [19] J. W. Pickering, T. B. Martins, M. C. Schroder & H.R. Hill, *Clinical Diagnostics Lab Immunol*, **9** (2002) 872-876.
- [20] M. Estevez, M. Alvarez & L. Lechuga, *Laser & Photonics Reviews* **6** (2012) 463-487.
- [21] M. B. F Suah, M. Ahmad & L.Y. Heng, *Sains Malaysiana* **45** (2016) 1795-1805.
- [22] W. Bogaerts, R. Baets, P. Dumon, V. Wiaux, S. Beckx, D. Taillaert & D. Van Thourhout, *Journal of Lightwave Technology* **23** (2005) 401-412.
- [23] H. T. Hattori, C. Jagadish, C. Seassal, S. Boutami, B. Ben Bhakir, E. Drouard, X. Letartre & P. Viktorovitch, *IEEE International Conference on Mathematical Methods in Electromagnetic Theory*, (2006) 35-40.
- [24] M. I. Newton, P. Roach & G.McHale, *Sensors* **8** (2008) 4384-4391.
- [25] S. Ballandras & E. Bigler, *IEEE Transactions on Ultrasonics, Ferroelectrics and Frequency Control* **45** (1998) 567-573.
- [26] F. A. Said, P. S. Menon, K. Tarumaraja, M. A. Mohamed, A. Abedini, S. Shaari, B. Y. Majlis & V. Retnasamy, *Proc. IEEE Regional Symposium on Micro and Nano Electronics (RSM)*, (2015) 1-4.
- [27] F. A. Said, P. S. Menon, S. Shaari & B.Y. Majlis, *Proc. International Conference on Intelligent Systems, Modelling and Simulation (ISMS)*, (2015) 242-245.
- [28] F. A. Said, P. S. Menon, S. Shaari & B.Y. Majlis, *International Journal of Simulation: Systems, Science and Technology* **16** (2015) 6.1-6.5.
- [29] D. Wu, W. Chien, C. Yang & Y. Yen, *Sensors and Actuators A: Physical* **118** (2005) 171-176.
- [30] O. Nagler, M. Trost, B. Hillerich & F. Kozlowski, *Sensors and Actuators A: Physical* **66** (1998) 15-20.
- [31] H. Tsai, D. Wu, T. Chiang & H. Chen, *Sensors* **9** (2009) 1394-1408.

- [32] A. Afifah Maheran, P. S. Menon, I. Ahmad & S. Shaari, *Materials Science in Semiconductor Processing* **17** (2014) 155-161.
- [33] H. Haroon, S. Shaari, P. S. Menon, H. Abdul Razak, M. Bidin, *International Journal of Numerical Modelling: Electronic Networks, Devices and Fields* **26** (2013) 670-679
- [34] C. Hamzaçebi, *Bio Resources* **11** (2016) 5987-5993.
- [35] K. A. Tarumaraja, P.S. Menon, F. A. Said, N.A. Jamil, A. A. Ehsan, S. Shaari, B.Y. Majlis & A. Jalar, *IEEE International Conference on Semiconductor Electronics (ICSE)*, (2016) 79-81.
- [36] K. A. Tarumaraja, P. S. Menon, F. A. Said, N.A. Jamil, S. M. Gan, S. Shaari & B.Y. Majlis, *IEEE Region 10 Conference TENCN*, (2017) 2698-2701.
- [37] K. A. Tarumaraja, P.S. Menon, S. Shaari, Ahmad G. Ismail & B.Y. Majlis, *Journal of Nanoelectronics and Optoelectronics*. **13** (2018) 839-845.
- [38] M. S. Phadke, *Quality Engineering Using Robust Design*, New Delhi, India: Dorling Kindersley and Pearson Education, (2008).
- [39] Y. Wu & A. Wu, *Taguchi Method for Method for Robust Design*. New York: ASME, (2000).
- [40] M. S. Phadke, *Quality Engineering Using Robust Design*, Lebanon USA: Prentice Hall, (1989).
- [41] S. EL-Moslamy, M. Elkady, A. Rezk & Y. Abdel-Fattah, *Scientific Reports* **7** (2017) 45297.
- [42] A. Mitra, M. Jawarkar, T. Soni & G. Kiranchand, *Procedia Engineering* **144** (2016) 77-84.
- [43] W. Y. Fowlkes & C. M. Creveling, *Engineering methods for robust product design: using Taguchi methods in technology and product development*. Lebanon, USA: Prentice Hall PTR, (1995).
- [44] F. Prieto, B. Sepulveda, A.Calle, A. Llobera, C. Domínguez, A. Abad, A.Montoya & L. M, *Nanotechnology* **14** (2003) 907-912.
- [45] Y. Joo, S. Song & R. Magnusson, *Optics Express* **17** (2009) 10606-10611.
- [46] P. Prabhathan, V. Murukeshan, Z. Jing & P. Ramana, *Optics Express* **17** (2009)15330-15341.
- [47] F. Kehl, D. Bischof, M. Michler, M. Keka & R. Stanley, *Photonics*. **2** (2015) 124-138.